

ISSN: (Print) (Online) Journal homepage: <https://www.tandfonline.com/loi/tbsd20>

Bioinformatic and computational analysis for predominant mutations of the Nrf2/Keap1 complex in pediatric leukemia

Dilara Fatma Akin-Bali, Khattab Al-Khafaji, Sedef Hande Aktas & Tugba Taskin-Tok

To cite this article: Dilara Fatma Akin-Bali, Khattab Al-Khafaji, Sedef Hande Aktas & Tugba Taskin-Tok (2021) Bioinformatic and computational analysis for predominant mutations of the Nrf2/Keap1 complex in pediatric leukemia, *Journal of Biomolecular Structure and Dynamics*, 39:12, 4290-4303, DOI: [10.1080/07391102.2020.1775702](https://doi.org/10.1080/07391102.2020.1775702)

To link to this article: <https://doi.org/10.1080/07391102.2020.1775702>



Published online: 16 Jun 2020.



Submit your article to this journal [↗](#)



Article views: 260



View related articles [↗](#)



View Crossmark data [↗](#)



Citing articles: 1 View citing articles [↗](#)



Bioinformatic and computational analysis for predominant mutations of the Nrf2/Keap1 complex in pediatric leukemia

Dilara Fatma Akin-Bali^a, Khattab Al-Khafaji^b, Sedef Hande Aktas^c and Tugba Taskin-Tok^{b,d}

^aFaculty of Medicine, Department of Medical Biology, Nigde Omer Halisdemir University, Nigde, Turkey; ^bFaculty of Arts and Sciences, Department of Chemistry, Gaziantep University, Gaziantep, Turkey; ^cVocational School of Health Services, Eskisehir Osmangazi University, Eskisehir, Turkey; ^dDepartment of Bioinformatics and Computational Biology, Institute of Health Sciences, Gaziantep University, Gaziantep, Turkey

Communicated by Ramaswamy H. Sarma.

ABSTRACT

The levels of reactive oxygen species (ROS) are tightly controlled and regulated by Nuclear Factor Erythroid-2-Like 2 (Nrf2) transcription factor, which is the main regulator of antioxidant responses and its suppressor protein Kelch-like ECH-associated protein 1 (Keap1). Our previous study has identified six novel changes in Nrf2/Keap1 pathway in pediatric ALL, which were described for the first time. These changes in the pathway are likely to alter the evolutionary process of amino acids and cause structural changes in the final products of genes. In this study, we aimed to compare the pathogenicity of eight determined mutations reported in our previous study by utilizing different programs with different algorithms and molecular dynamics simulation. Since it is too difficult to handle each existing mutation in a wet laboratory, *in silico* methods may give suggestion to choose the important mutations for further analysis and to establish the appropriate patient population and conduct wet laboratory studies. For this purpose, four different algorithms were used to evaluate the effects of single amino acid mutation. In addition, root-mean-square deviation, root-mean-square fluctuation and free-energy landscape analyses were performed to observe stability, flexibility and energetically favorable conformations, respectively, for each amino acid mutation. As a result, our study emphasizes the importance of Keap1 mutations in pediatric ALL Nrf2/Keap1 pathway, a total of eight mutations, two of which were shown for the first time in our study. Especially the mutations in the Keap1 Broad-Complex, Tramtrack and Bric-à-brac domain are worthy of attention.

ARTICLE HISTORY

Received 1 April 2020
Accepted 25 May 2020

KEYWORDS

Acute lymphocytic leukemia; molecular dynamics simulation; Nrf2/Keap1 pathway; ROS; mutation; pediatric

Introduction

ALL is a malignant transformation of lymphoid precursor cells within the bone marrow and has poor prognosis after relapse (Carroll & Raetz, 2012; Mullighan, 2014; Mullighan & Downing, 2009; Pui & Evans, 1998; Zhang et al., 2019). Oxidative stress has been associated with many types of cancer including ALL and found to be important for disease progression (Abdul-Aziz et al., 2015; Kerins & Ooi, 2018; Leinonen et al., 2015). Nuclear Factor Erythroid-2-Like 2 (Nrf2)/Kelch-like ECH-associated protein 1 (Keap1) pathway has an important role in the regulation of oxidative stress and displays abnormally high genomic and transcriptomic alterations in most cancers (Baird & Dinkova-Kostova, 2011; Kansanen et al., 2013; Kaspar et al., 2009). Although oxidative stress-related pathway mutations are not driver mutations, it would not be right to leave them out of pediatric ALL assessment due to stated reasons (i) among leukemia groups, as pediatric therapy regimens are more aggressive and continuous. Children undergoing treatment for ALL receive multi-agent chemotherapy drugs like cytosine arabinoside, doxorubicin, cyclophosphamide and methotrexate that cause the

production of free radicals. In view of remarkably higher reactive oxygen species (ROS) levels in pediatric ALL, (ii) increased levels of mutation in cells is correlated with pathologically increased ROS levels (iii) and increased genomic instability; double-stranded DNA fractures are correlated with ROS accumulation; (iv) point mutations can cause translocations in leukemic cells and disrupted cellular redox compensation mechanism (Chu et al., 2018; Kansanen et al., 2013; Kim & Keum, 2016; Suzuki & Yamamoto, 2015; Zhang, 2010). Our previous study aimed to find out the mutations in this pathway in pediatric ALL patients for the first time.

As cytogenetic alterations and molecular abnormalities are frequent changes seen in ALL, there have been several molecular markers to predict prognosis and classify risk. Also, there have been a few identified genetic alterations with clinical significance and different mutation distribution (Wang et al., 2016; Zhang et al., 2019). However, the effect of this different mutation/single nucleotide polymorphism (SNP) distribution on protein structure as a result of DNA-based analyses have not been investigated in detail by *in silico* methods; thereby, its effect on the possible pathogenesis of

CONTACT Dilara Fatma Akin-Bali ✉ dilarafatmaakin@gmail.com; dilarabali@ohu.edu.tr Faculty of Medicine, Medical Biology, Nigde Omer Halisdemir University, Nigde, Turkey; Tugba Taskin-Tok ✉ ttaskin@gantep.edu.tr; taskin.tugba@gmail.com; Faculty of Arts and Sciences, Department of Chemistry, Gaziantep University, 27310, Gaziantep, Turkey.

the predicted disease and its possible characteristics to be used in the diagnosis have not been reflected in the clinic. Considering our previous data and especially the six novel changes, the current study was designed to investigate the effect of identified mutations on the proteins of Keap1 assemblance and Nrf2 peptide.

Patients and methods

Patients and mutations screening

Thirty-pediatric ALL patients have been tested. All patient information, demographic-clinical information, method steps and study results, is detailed in our previous study. In order to identify mutations in the Nrf2/Keap1/Nuclear factor kappa-B1(NF- κ B1)/phosphotyrosine-independent ligand for the Lck SH2 domain of 62 KDa (p62) pathway, the coded regions of the relevant genes have been extensively screened by DNA sequence analysis in 30 children diagnosed with pediatric ALL (Akin-Bali et al., 2020).

In silico analysis of the Nrf2/Keap1 pathway mutations

Mutation analysis

Polymorphism Phenotyping v2 (PolyPhen-2), screening for non-acceptable polymorphisms (SNAP), Cancer-specific High-throughput Annotation of Somatic Mutations (CHASM) and Variant Effect Scoring Tool (VEST) automatic tools were performed to predict the possible impact of amino acid substitutions on the structure and function of a human protein using structural and comparative evolutionary considerations.

PolyPhen-2 calculates the functional description of SNPs, maps coding SNPs to gene transcripts, extracts protein sequence annotations and structural characteristics and constructs conservation profiles. The program is the most prominent tool based on both sequence and structural information. It estimates the probability of the missense mutation being damaging based on a combination of all these features and provides both a qualitative prediction (probably damaging, possibly damaging, benign or unknown) with a score (Adzhubei et al., 2010, 2013; Walters-Sen et al., 2015).

SNAP is a trained classifier that is based on a machine learning device called 'neural network'. It distinguishes between effect and neutral variants/non-synonymous SNPs by taking a variety of sequence and variant features into account. SNAP comprises evolutionary constraints, structural features and protein annotation information. The most important single feature for SNAP prediction is conservation in a family of related proteins as reflected by Position-Specific Independent Counts scores. However, the installation of this automatic tool is quite complex (Bromberg & Rost, 2007).

CHASM differentiate from PolyPhen-2 and SNAP being the cancer specific tool. The program is trained on cancer mutations from The Catalogue of Somatic Mutations in Cancer (COSMIC) and other cancer-related resources. It relies on training sets, structure, conservation and annotation. It uses

49 predictive features ranging from exon conservation to UniProt annotation and frequency of missense change type in COSMIC (Carter et al., 2009; Tate et al., 2019; Wong et al., 2011).

In addition, the last program we used is VEST. It is a machine learning method that predicts the functional significance of missense mutations based on the probability that they are pathogenic (Carter et al., 2013; Douville et al., 2016).

Evolutionary conservation analyzes of the detected mutant amino acids were evaluated among different species (*Homo sapiens* to *Xenopus tropicalis*).

Molecular dynamic analysis

Molecular dynamic (MD) simulation is a method of choice that has been applied widely in exploring mechanisms of conformational changes in protein mechanisms caused by mutations. MD simulation studies are widely applied to explain mechanisms and functions due to mutations. In *in vivo* experimental research, the mutations were determined; therefore, the MD simulation was used the behaviors to explain the effect of single mutations on dynamical behavior of keap1 proteins at atomic levels (Ganesan & Ramalingam, 2019; Liu & Yao, 2010), which have been considered difficult by experimental procedures (Khan et al., 2019).

MD simulation has a vital role in the investigation of structural and thermodynamical stability of single mutations within Keap1 proteins and Nrf2 peptides (Kumar, Gupta, et al., 2019). It provides the conformational changes with the time scale, from where we can find that the wild type (WT) or mutated protein is stable or not (Shukla et al., 2019). In this study, MD simulations were executed for selected targets in both WT and single mutated proteins. MD simulation was performed using GROMACS 2018.1 package (Abraham et al., 2015), with Charmm 27 force field for all atoms (Bjelkmar et al., 2010). All systems were solvated with three-point transferable intermolecular potential, and their charges were neutralized by adding Na or Cl ions. The next step, energy minimization, was proceeded by the steepest descent algorithm at a tolerance value of 1000 kJ/mol nm, then followed by equilibration with position restraint on the protein molecules for 0.1 ns using constant number, volume and temperature and constant number, pressure and temperature ensembles. Particle Mesh Ewald summation was employed to assess all the electrostatic interaction. After all the optimizations, the simulation was performed without any restraint on the protein molecules or ligand for 10 ns to determine the stability. Finally, MD simulation was performed at a timescale of 10 ns and in 5,000,000 steps (time step of 0.000002 ns). Then, the trajectories were analyzed using gmx rms to estimate the root-mean-square deviation (RMSD) and gmx rmsf to determine the root mean square fluctuation of residues (RMSF). In addition, the free-energy landscape (FEL; Frauenfelder et al., 1991) was obtained using gmx sham tool, which is based on the values of principal component analysis (Amadei et al., 1996) from running gmx anaieg and gmx covar tools.

Table 1. Pathogenic mutations of the Nrf2/Keap1 pathway in patients with pediatric ALL.

No	Gene	Nt alteration	Rs Number	Alteration type	Localization	AA position	Number of patients carrying changes	Previously determined tumor type	Clinical significance			
									Polyphen-2	SNAP	CHASM	VEST
C1	<i>Keap1</i>	c.432 C > A	Novel	Silent nucleotide variant	BTB Domain	p.S144S	1	Present Study	Probably damaging 0.97	Neutral	Neutral	Neutral
C2	<i>Keap1</i>	c.475G > A	COSM6196644	Missense mutation	BTB Domain	p.A159T	3	Ovarian cancer	Somatic mutation score (pathogenic) 1.00	Neutral	0.1034	0.0039
C3	<i>Keap1</i>	c.474 T > C	COSM4131169 rs1048287	Synonymy nucleotide variant	BTB Domain	p.G158G	1	Thyroid cancer, Urinary tract cancer	Somatic mutation score (nonpathogenic) 0.06	Neutral	Neutral	Neutral
C4	<i>Keap1</i>	c.665delA	Novel	Missense mutation	IVR Domain	p.N222T	2	Present Study	Benign (nonpathogenic) 0.022	Neutral	0.6714	0.2503
C5	<i>Keap1</i>	c.1692_1693insT (insertion)	COSM6930460	Frameshift insertion	Keich repeats	p.R565fs*1	1	Lung cancer, AML	Somatic mutation score (pathogenic) 0.90	Effect	0.4722	0.1239
C6	<i>Keap1</i>	c.438C > T	COS5609243	Silent mutation	BTB Domain	p.S146S	1	Malignant melanoma	Somatic mutation score (pathogenic) 0.83	Neutral	Neutral	Neutral
C7	<i>Keap1</i>	c.361G > A	rs1040448829 COSM6967929	Missense mutation	BTB Domain	p.E121K	11	Pancreatic cancer	Somatic mutation score (pathogenic) 0.68	Neutral	0.0608	0.1955
C8	<i>Nrf2</i>	c.90T > G	rs770501791	Silent mutation	ETGE Domain	p.L32L	1	NA	UNK	Neutral	Neutral	Neutral

UNK: unknown; NA: not available; SNP: single nucleotide polymorphism; BTB: broad complex/tramtrack/briç a brac; AML: acute myeloid leukemia; C: change.

Results

Results of mutation analysis

The variants identified in the study and their descriptive features are given in detail in Table 1. In our previous study where we received our experimental data, mutation detection from DNA samples of 30 pediatric ALL patients was performed with the Sanger DNA sequence analysis system. As a result of mutation analysis in four genes on the Nrf2/Keap1/NF- κ B1/p62 signaling pathway, 17 changes (12 nucleotide changes, 2 deletion mutations and 3 insertions) were detected. Eleven of these changes have been previously registered in the Human Gene Mutation Database e-database, and six have been identified for the first time in our previous study (Akin-Bali et al., 2020). Table 1 summarized characterization of detected mutations in pediatric ALL patients. Schematic representation of domain architecture of the proteins and all mutations found in pediatric ALL are shown in Figure 1.

Bric-à-brac (BTB) domain of Keap1 promotes Nrf2 ubiquitination and subsequent proteasomal degradation and creates a binding site for Cullin 3 (Cul3)-E3-dependent ubiquitin ligase complex, which suppresses Nrf2 (Mitsuishi et al., 2012; Shibata et al., 2008). In our previous study where the data of this article was provided, two missense (p.E121K and p.A159T) three silent (p.S144S, p.S146S, p.G158G) mutations were detected on this domain (Akin-Bali et al., 2020).

Changes detected in the Keap1 gene are above the intervening region (IVR) and BTB domains that are functional for the protein of the gene. The p.N222T missense mutation was detected on the Keap1 IVR domain, and there is a conserved nuclear export signal sequence on this domain, which is important for the localization of Keap1 in the cytoplasm.

Using the 'Multiple sequence alignment' option in the PolyPhen-2 e-database, amino acid sequences affected by the detected mutations were compared between 13 different species. As a result, it was determined that Keap1 p.E121K, p.A159T, p.N222T and p.R565M missense mutations changed amino acids in the critical point that have been preserved between species, from *H. sapiens* to *Xenopus laevis*. According to the results of PolyPhen-2, because the pathogenic scores of p.E121K and p.A159T missense mutations in the Keap1 domain are near 1, the mutations were determined as probably pathogenic (Figure 2).

In addition, although p.E121K, p.A159T and p.R565M mutations had been registered to COSMIC database before, the p.N222T missense mutation that we reported in our previous study was identified for the first time. Neh2 domain, is the regulator domain, contains seven lysine residues responsible for arranging to help the two binding areas (ETGE and DLG motifs) for the stability of Nrf2 besides its role in ubiquitin conjugation. p.L30L change, which was detected in Nrf2 gene, is on the domain of Keap1 binding domain: ETGE-Neh2. According to the prediction analysis on SNAP software, p.E121K, p.A159T and p.N222T missense mutations and p.S144S, p.S146S and p.G158G silence mutations were detected as neutral, and p.R565M missense mutation was detected as affected for protein in Keap1 (Figure 3).

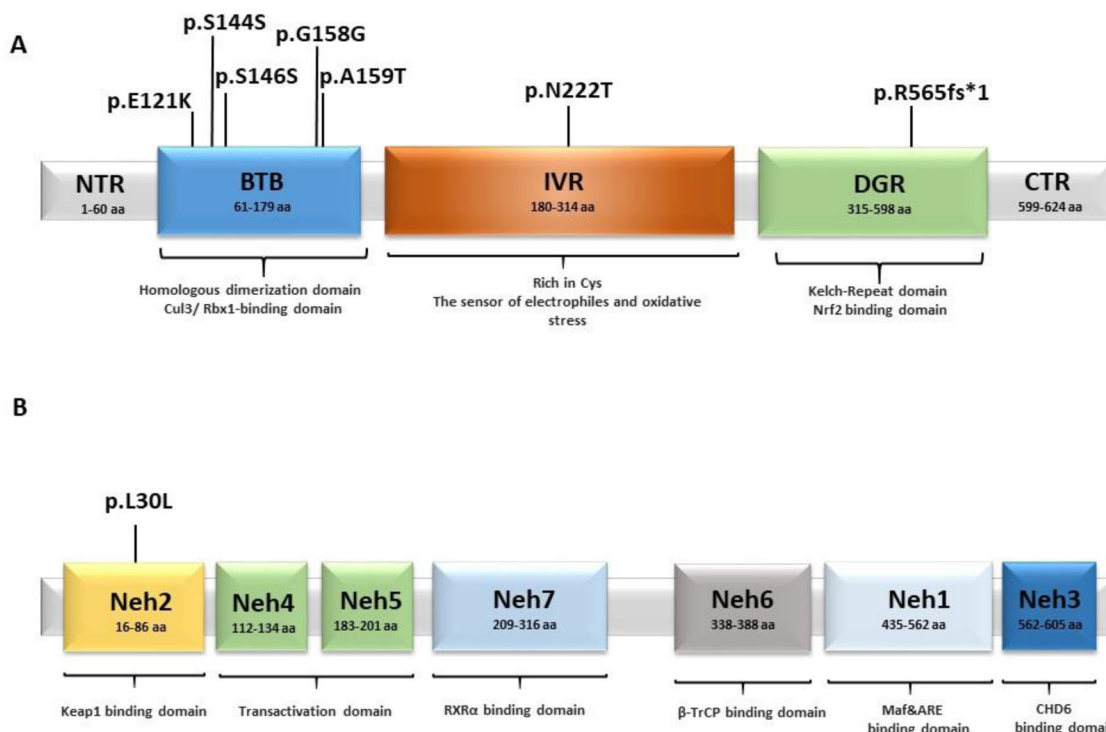


Figure 1. Schematic representation of domain architecture of the Keap1 (A) and Nrf2 (B) proteins and mutations found in pediatric ALL.

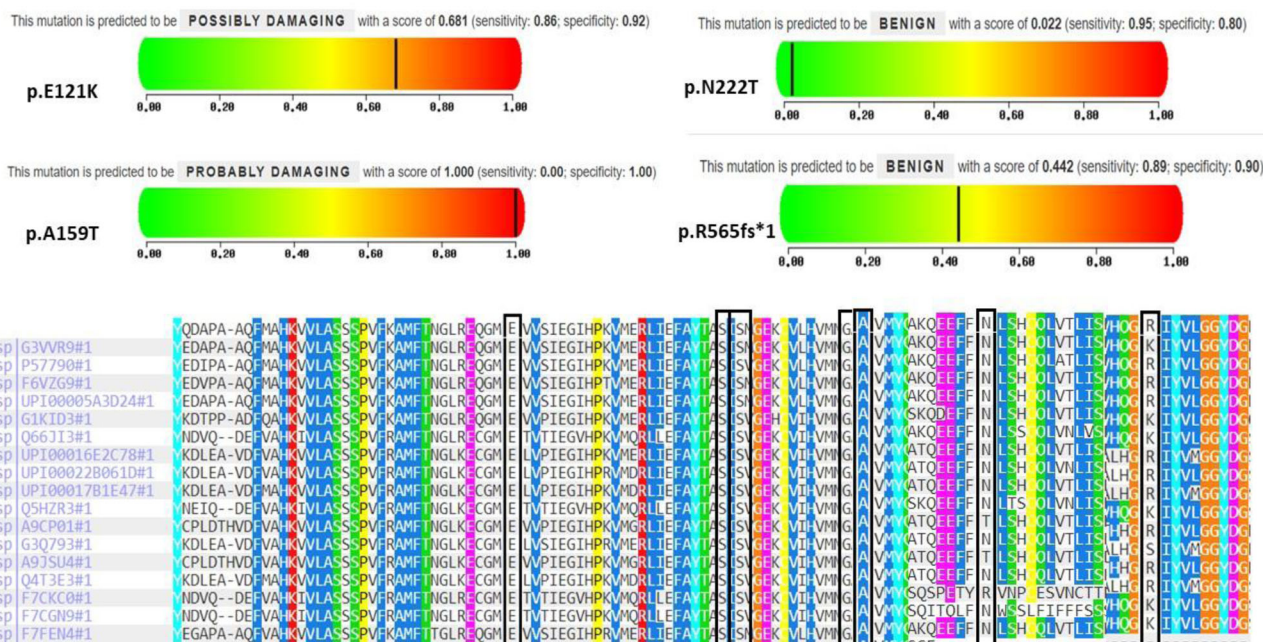


Figure 2. Keap1 Pathogenic mutations associated variations predicted by predicted by Poly-phen software.

Results of MD simulation

MD simulation represents a groundbreaking method to investigate the dynamic behavior of proteins and the effect of mutations on the behavior of understudied proteins. The 10-ns time scale of MD simulations was running for BTB domain and its mutants (E121K, S144S, S146S, G158G and A159T), IVR domain with its mutant (N222T) and DGR domain in addition to the Neh2 domain with its mutant. Throughout the study, two different parameters as RMSD

and RMSF will be used to analyze the MD simulation trajectories.

Figure 4 was shown that Ribbon and surface images of the structure of Nrf2/Keap1 complex.

Structural stability of systems

The RMSD has emerged as a powerful tool in the investigation of deviation caused by single mutation on general

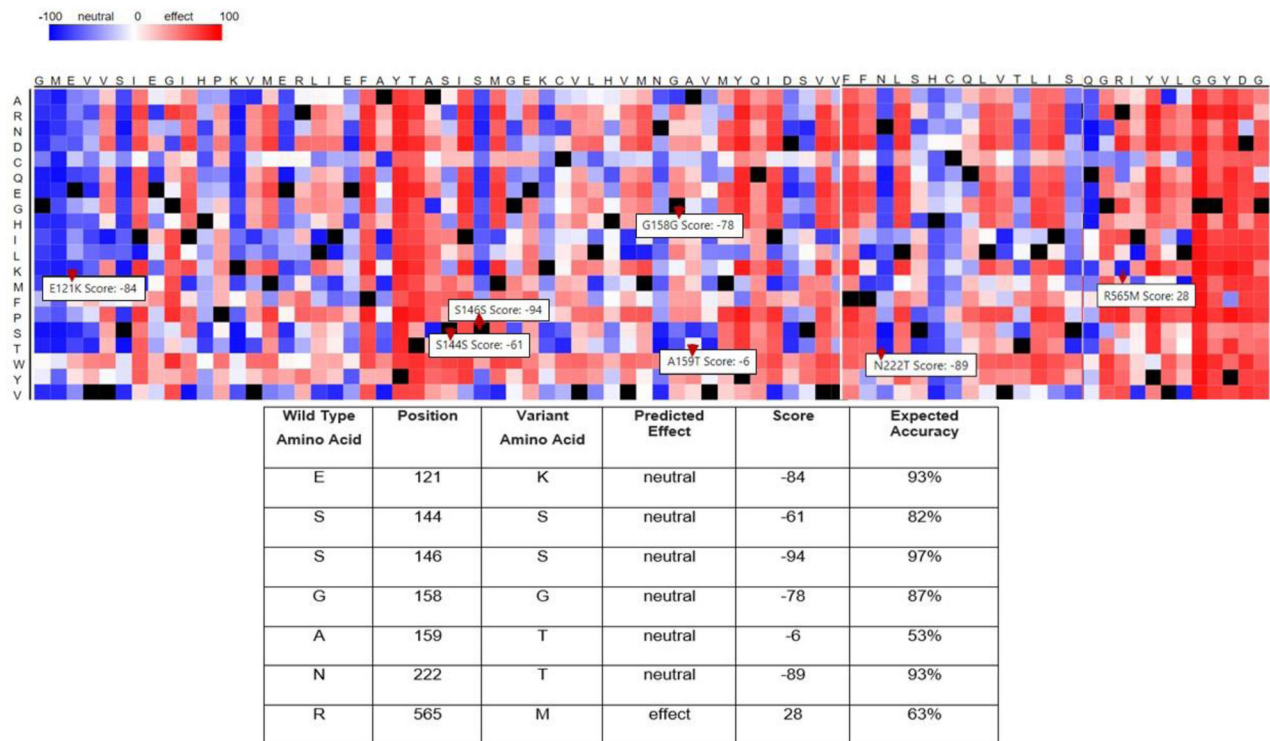


Figure 3. *Keap1* Pathogenic mutations associated variations predicted by predicted by SNAP software.

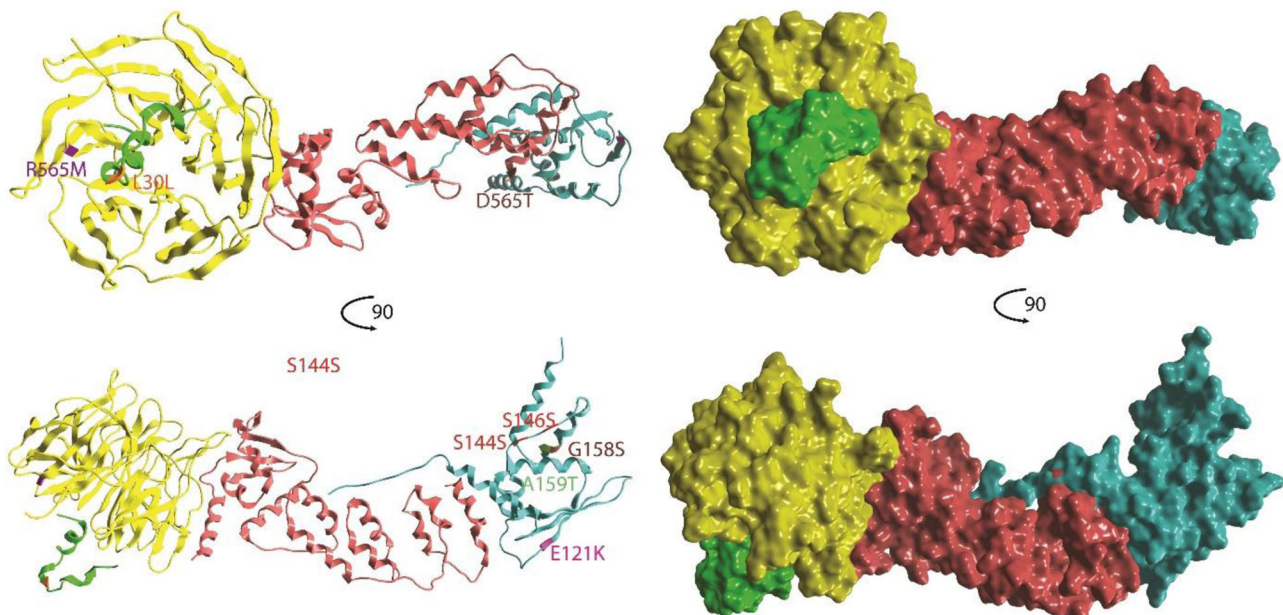


Figure 4. Ribbon and surface images of the structure of Nrf2/Keap1 complex, illustrates the amino acid locations of mutations. DGR domain (yellow), BTB domain (indianred), IVR domain (cyan) and Neh domain (green).

behavior of native configuration. The RMSD of protein backbone atoms of BTB domain of Keap1 besides its mutants were measured to determine the converging of MD trajectories files between the WT models, and their mutants were calculated using crystal structure as reference and protein backbone atoms for least fitting (Figure 5). All the RMSD values for WT and determined mutation of BTB domain (Figure 5(A)) were calculated using crystal structure as reference and protein backbone atoms for

least fitting. The mean values of RMSD of the WT, E121K, S144S, S146S, G158G and A159T models were 0.44, 0.36, 0.32, 0.35, 0.39 and 0.36 nm, respectively (Figure 5(A)). This result is relatively counterintuitive, because WT has the highest RMSD value compared to mutant models. It can be seen in Figure 5(B) that the continuous increase in the RMSD distribution shifted to the left axes with the largest distance. Another significant finding is the configuration mutations from L-configuration to D-configurations

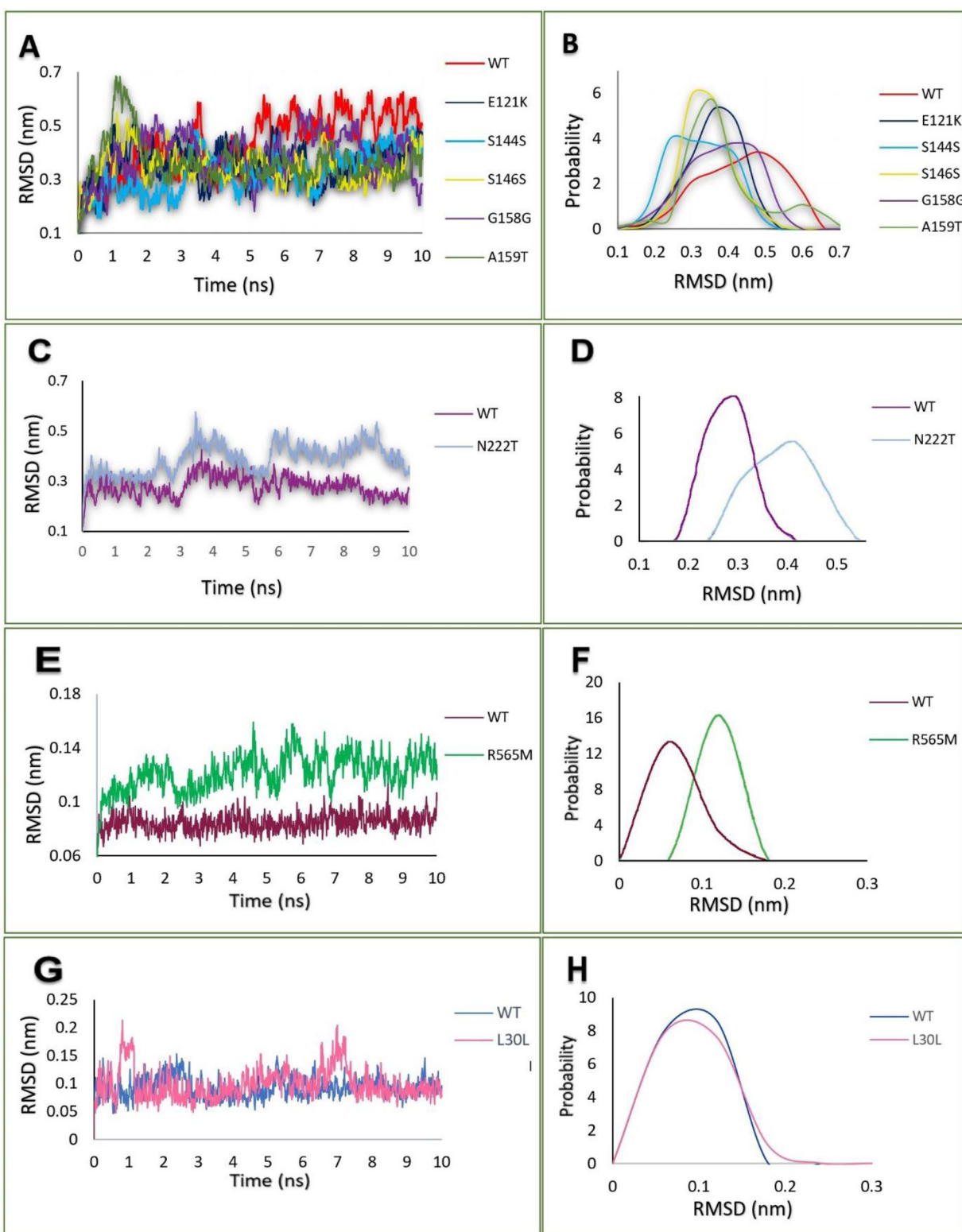


Figure 5. (A) RMSD evolutions of protein backbone atoms with simulation time in WT and mutants' systems of BTB domain; (B) Probability distribution of RMSD values BTB domain; (C) RMSD evolutions of protein backbone atoms with simulation time in WT and mutant's systems of IVR domain; (D) Probability distribution of RMSD values of N-IVR domain; (E) RMSD evolutions of protein backbone atoms with simulation time in WT and mutant's systems of DGR; (F) Probability distribution of RMSD values of DGR; (G) RMSD evolutions of protein backbone atoms with simulation time in WT and mutant's systems of NrF peptide; (H) Probability distribution of RMSD values of Neh2 domain.

in serie in 146 led to increased rigidity compared to the other mutated models, which showed higher probability (0.36) and narrower distribution around the same RMSD.

In the figure (Figure 5(C)), the RMSD values of native and mutant IVR domain showed a nearly similar fashion of deviation until 8.5 ns from their starting structure. The RMSD mean value was 0.26 and 0.32 nm during the simulations,

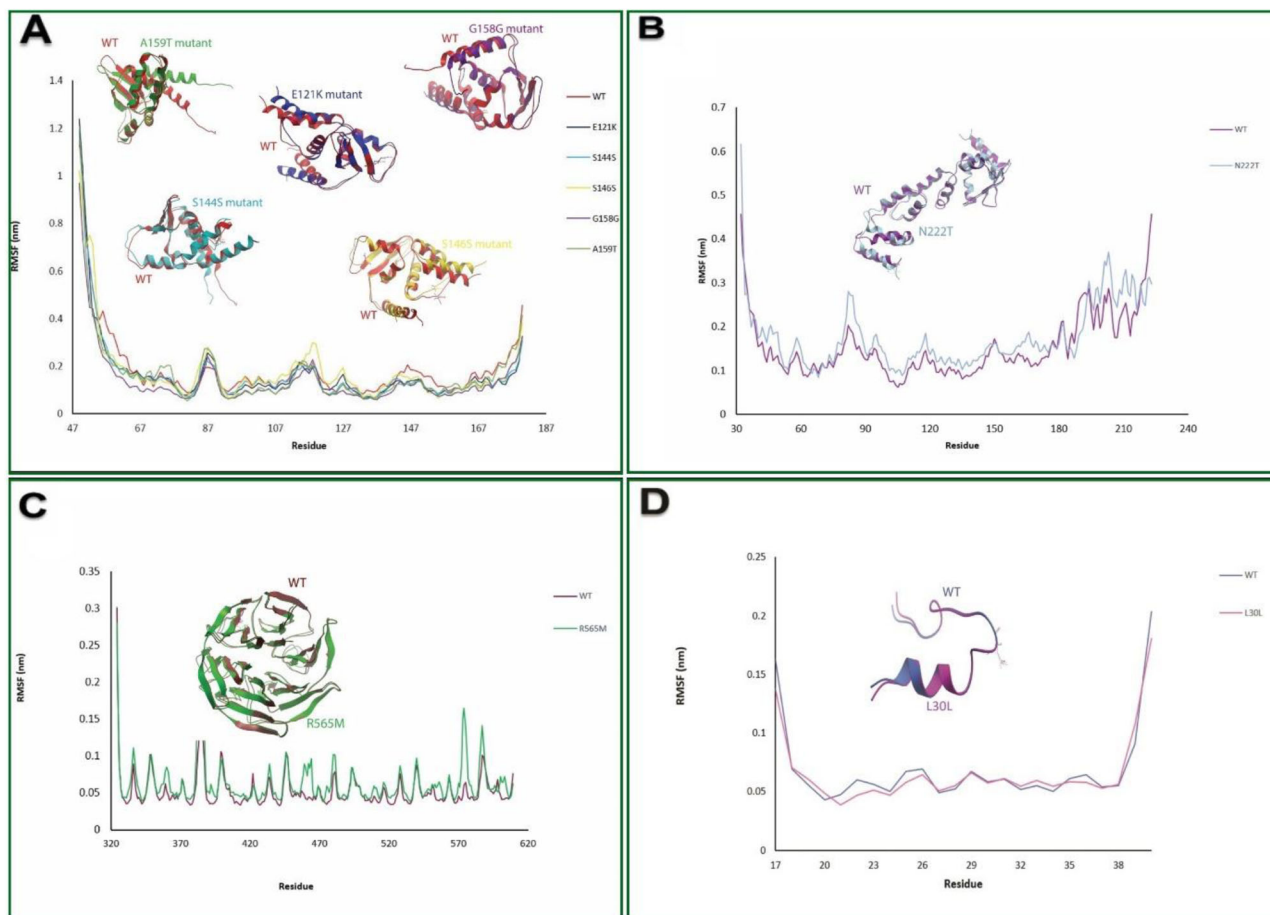


Figure 6. (A) RMSF of protein backbone atoms with simulation time in WT and mutants' systems of BTB domain; (B) RMSF of protein backbone atoms with simulation time in WT and mutant' systems of IVR domain; (C) RMSF of protein backbone atoms with simulation time in WT and mutant' systems of DGR domain; (D) RMSF of protein backbone atoms with simulation time in WT and mutant' systems of Neh2 domain.

and the mutant showed more deviation and attained approximately 0.57 nm of backbone RMSD at 3.47 ns, while the native structure maintained an RMSD value of 0.2 to 0.4 nm. Between 8 and 8.9 ns, the native structure showed a decrease from 0.36 to 0.23 nm and attained an RMSD value of 0.245 nm at 10 ns. The mutant protein increased from 0.38 to 0.53 nm between 8 and 8.9 ns. After then, a rapid decrease was seen in the RMSD of mutant from 0.53 to 0.32, despite the mutant retained maximum deviation until the end. Figure 5(D) shows that the RMSD distribution of the mutant system shifted in the right direction with broad range, while the RMSD distribution of WT protein was sharper and had higher probability (0.230).

Similarly, the monitored RMSD of DGR domain's backbone showed that the mean values of RMSD of the backbone of WT and R565M mutant system were 0.084 and 0.121 nm, respectively (Figure 5(E)). The RMSD value retained fluctuation onward between 0.0723 and 0.107 nm, but for mutant protein, the range of fluctuation was from 0.99 to 0.15 nm. What stands out in Figure 5(F) in the distribution of RMSD epitomize is the shifting of RMSD of mutant protein to the right due to the mutation in 565 amino acid with methionine.

The RMSD value mutant (L30L) was found to be more stable compared to that of WT (Neh2 domain). The mutant Neh2 domain (L30L) attained stable conformations in 10 ns

as shown in Figure 5(G), with two short drifts at ~ 1 and ~ 7 nm as compared to the RMSD value of WT. Figure 5(H) displays the distributional probability of the RMSD of WT and mutant of Neh2 domain, which reflects no significant differences.

Structural flexibility

Analysis of the flexible regions based on gmx RMSF results showed the average position of fluctuations of all the backbone atoms of the amino acid residues with respect to the WT structures. The RMSF plot showed a higher fluctuation in WT of BTB domain except for loop regions (74–78), (85–90) and (116–121) compared to mutant models of BTB domain, (Figure 6(A)). A noticeable increase in fluctuation is apparent in the loop region (116–121) in Figure 6(A). From the data in Figure 6(A), it is clear that the RMSF values of G158G have the lowest fluctuation. Furthermore, the RMSF range of the WT of BTB domain is between 0.43 and 0.088 nm, and the range of the mutants is 0.61–0.104 nm.

From the RMSF plot (Figure 6(B)), we can see that N222T mutant of IVR domain shows more instability compared to the WT protein, and it is opposite to the mutations effect inside of BTB domain. The terminal region (221–223) of WT showed great fluctuations. The RMSF graph (Figure 6(C)) indicated that the mutant protein structure of DGR domain

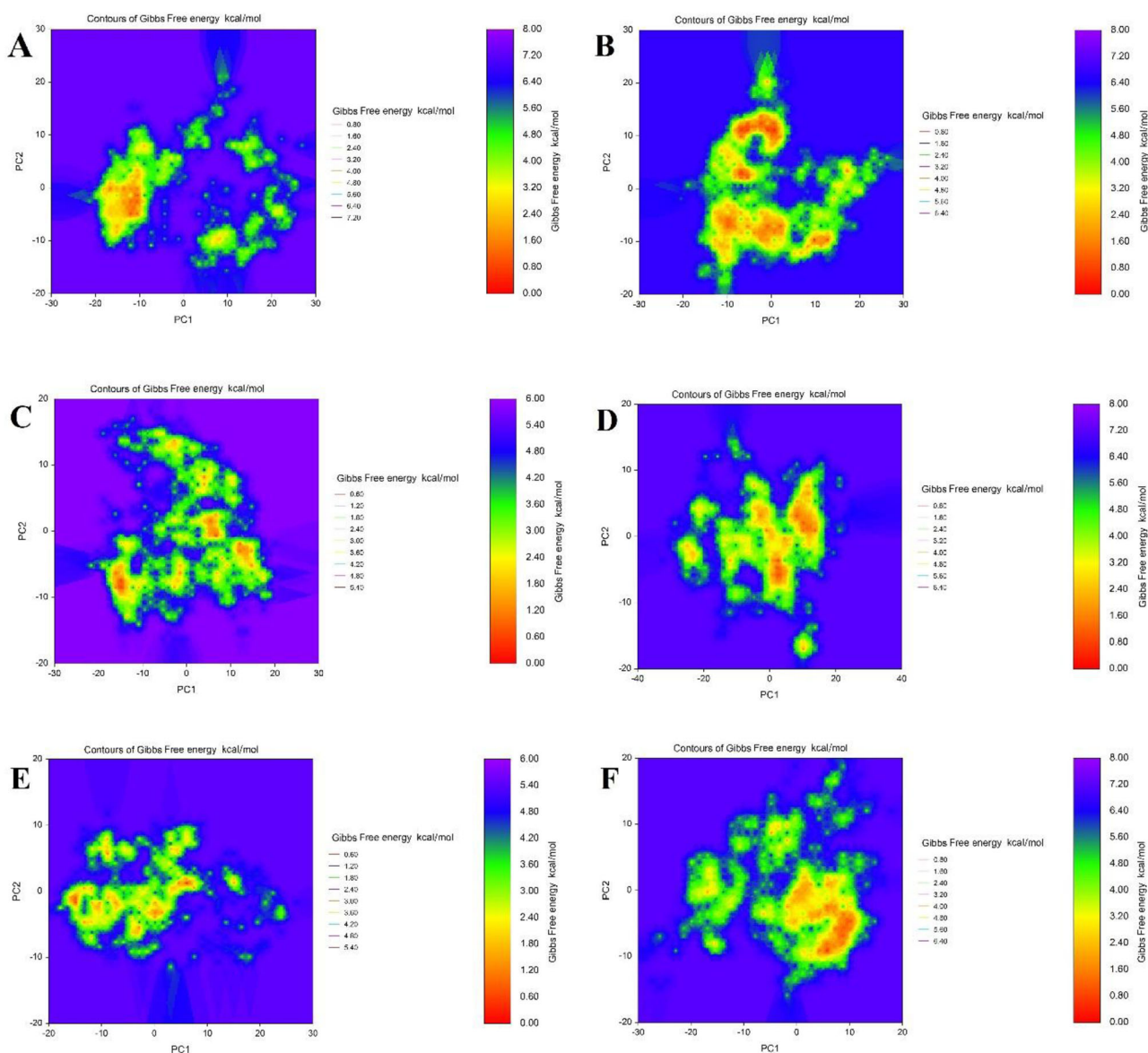


Figure 7. Gibbs free energy landscape calculated from PC1 and PC2 for BTB domain (A) WT, (B) E121K, (C) S144, (D) S146, (E) G158G and (F) A159T mutants.

showed significantly higher fluctuations than the native protein structure. Major changes were observed in regions of 384–387 and 573–575 near the active site (residues 170–210) and in the C-terminal region (residues 400–427) of mutant protein (Figure 6(C)), suggesting the increased flexibility caused by the R565M mutation. Moreover, backbone RMSF of mutant Neh2 domain displayed identical fluctuations for WT of Neh2 domain (Figure 6(D)).

Free-energy landscape

Information on FEL helps one determine the energetically favorable conformations (Narang et al., 2018). The global energy minima of the conformational states are shown in reddish orange. Figure 7 shows the FEL of (A) WT of BTB domain and its mutants. As can be seen from the figure, WT of BTB domain displayed a single dominant minimum energy basin observed to be associated with its conformational state

broad minimum energy basin with one of the lowest energy conformations (reddish orange). The A159T mutation in the (Figure 7(F)) mutation also contains a clear single point of lowest Gibbs energy, but with single lowest energy, and it is much broader than the basins of WT. However, it contains two well-characterized minimum energies for the S146S mutation (Figure 7(D)) and two broad minimum energy regions and two narrow minimum energy regions for the E121K mutation. In the case of S144S and G158G, there is no well recognized minimum region, and this represents the general direction of destabilization of S144 and G158G, even though they contain the minimum energy spots. Based on the results of FEL in Figure 7, all the five mutants of BTB domain showed random motion and were less energetically favored.

For furthermore investigation, the correlation of atomic movement was calculated by gmx covar, and the covariance matrix was obtained. Covariance values can be positive or negative, which provides information about the cooperativity

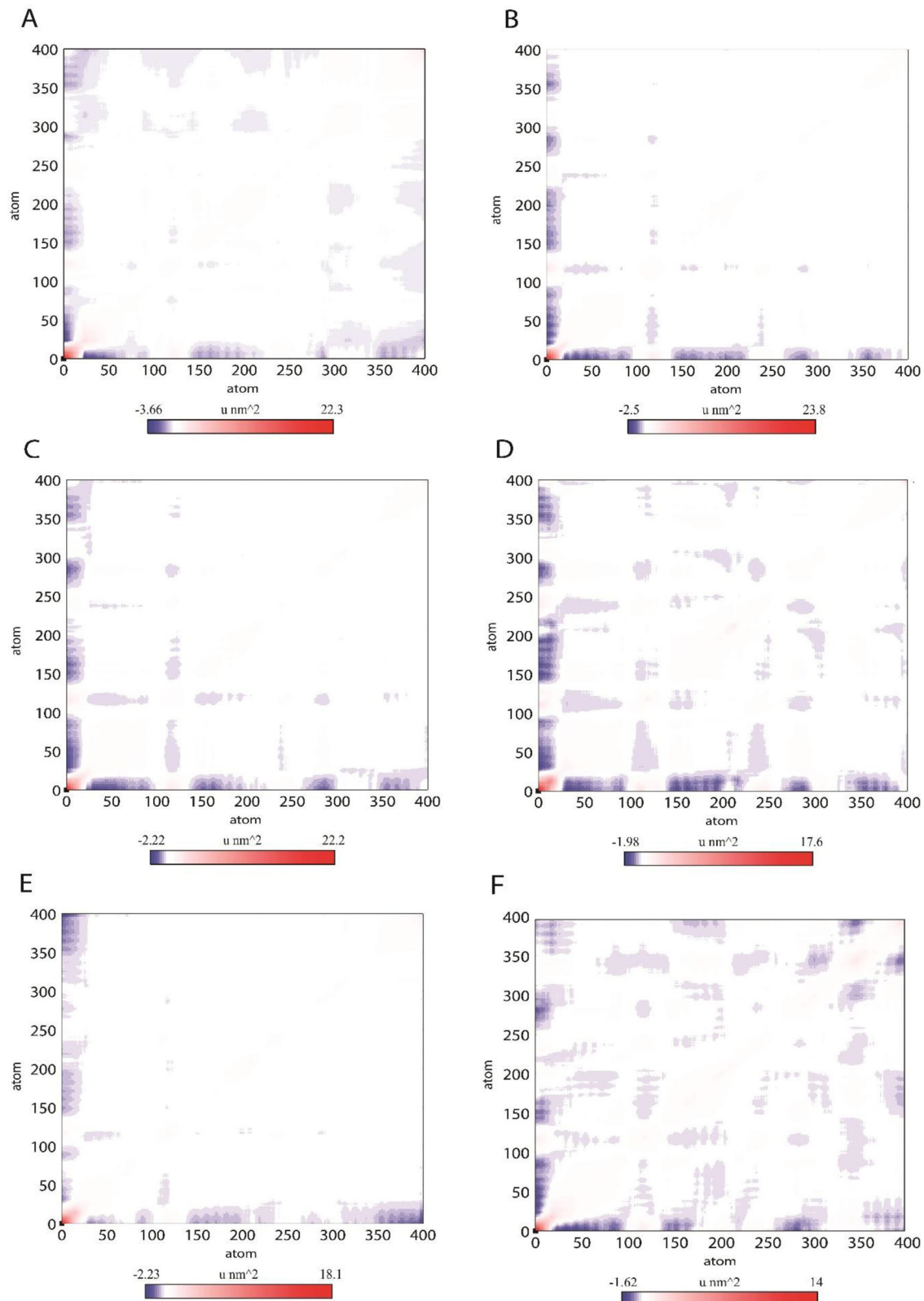


Figure 8. Covariance matrix plot of BTB domain of Keap1 (A) WT, (B) E121K, (C) S144, (D) S146, (E) G158G and (F) A159T mutants.

of motion. All diagonal elements of the symmetric $3N \times 3N$ covariance matrix were summed and termed as trace value, which provides information about the measure of total variance (Figure 8). The trace values calculated for the WT of E121K, S144S, S146S, G158G and A159T were found to be 24.56 nm^2 , 20.14 nm^2 , 19.47 nm^2 , 22.11 nm^2 , 16.74 nm^2 and

19.67 nm^2 , respectively. Higher trace value of WT and A182P related to the WT suggested an association with the enhanced flexible behavior of BTB domain. For the IVR domain, it can be seen from Figure 9(A) that WT has broader and lower free energy region compared to N222T mutant. FEL analysis indicates that N222T has thermodynamically less

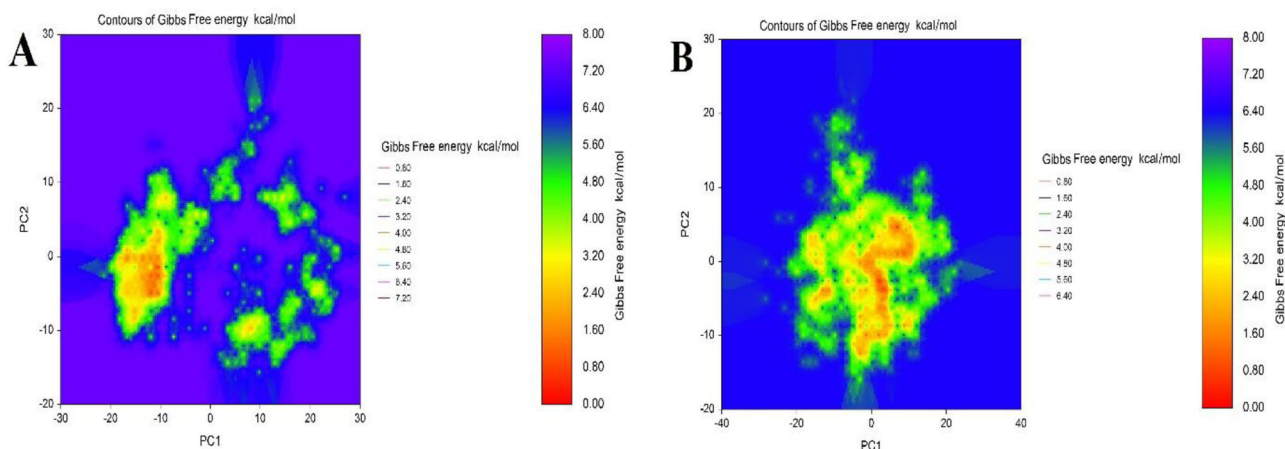


Figure 9. Gibbs free energy landscape calculated from PC1 and PC2 for IVR domain (A) WT and (B) N222T mutant.

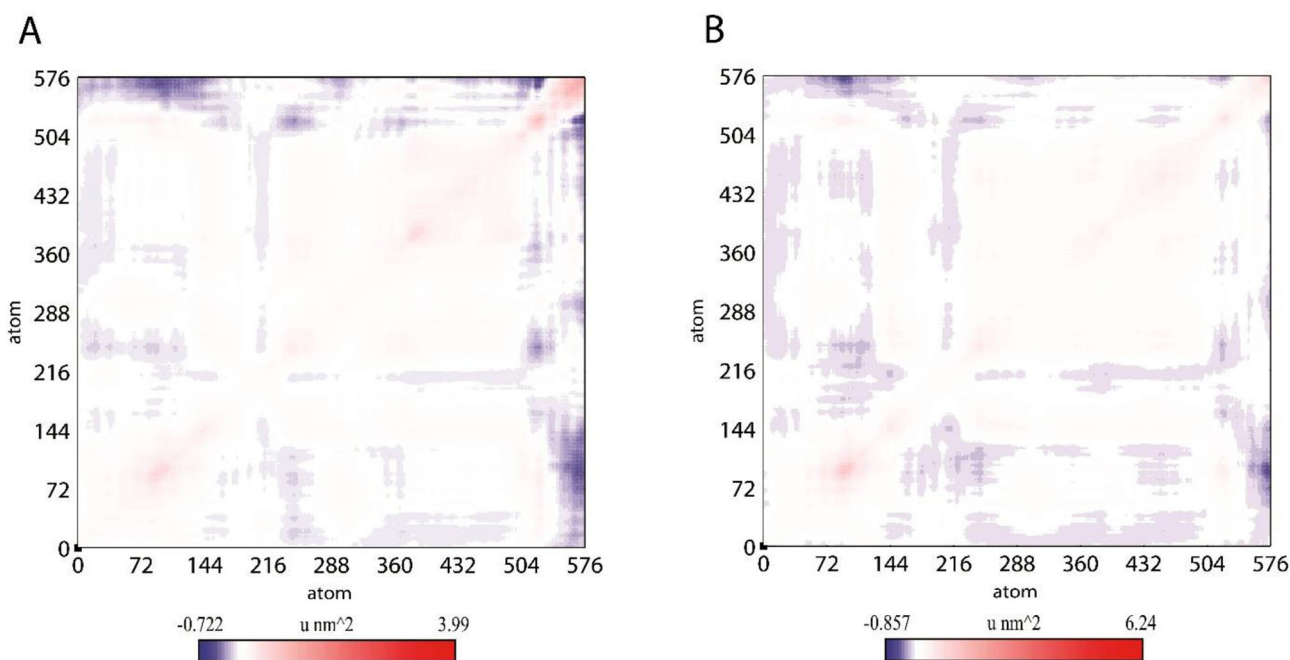


Figure 10. Covariance matrix plot of N-terminal domain of Keap1 (A) WT and (B) N222T.

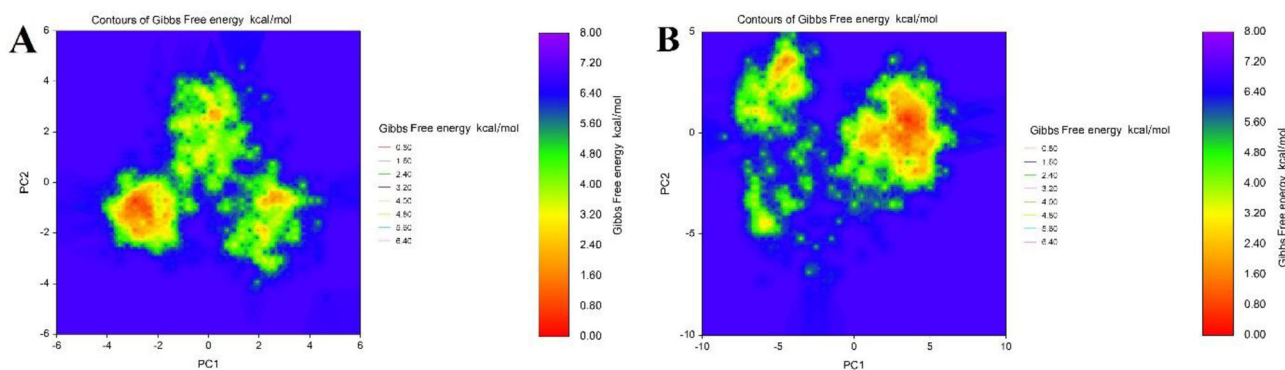


Figure 11. Gibbs free energy landscape calculated from PC1 and PC2 for DGR domain (A) WT and (B) R565M mutant.

stable conformations. Also, it can be seen in Figure 10 that the mutation of N222T drove to increase the flexibility of IVR where the positive correlation increased from 18.9008 to 22.2634 nm².

Interestingly, it is clear from Figure 11(A,B) that there is a significant enhancement in the energetic stability for the Kleck domain of Keap1 after mutation at 565 with methionine, despite that RMSD and RMSF revealed WT to be much

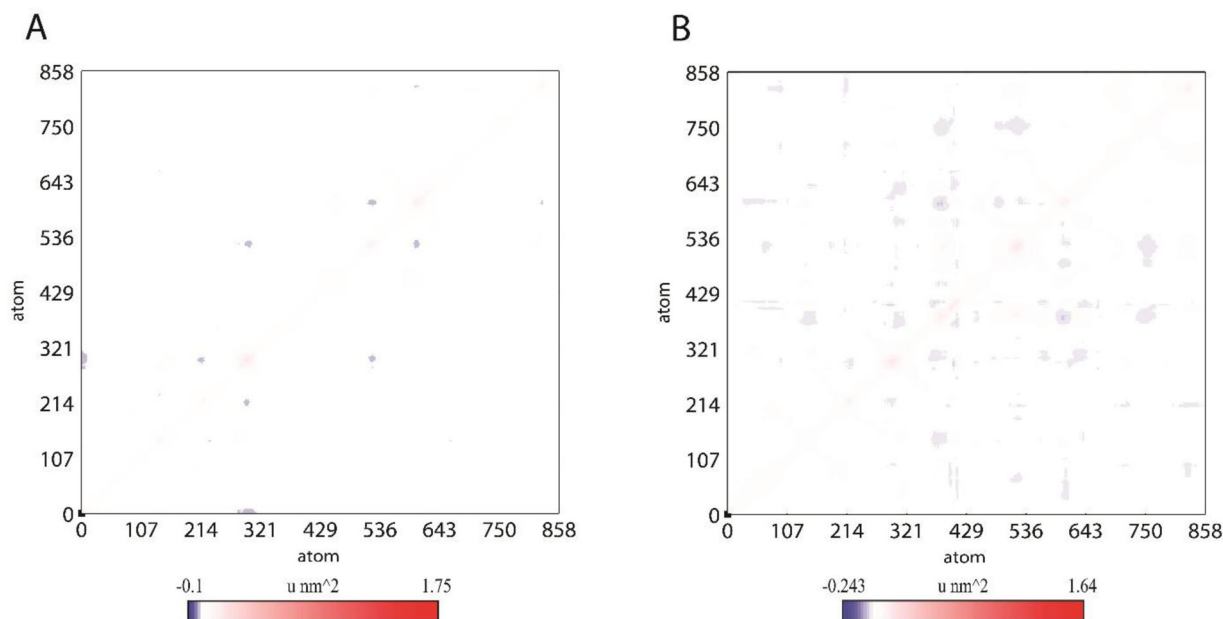


Figure 12. Covariance matrix plot of DGR domain (A) WT and (B) R565M.

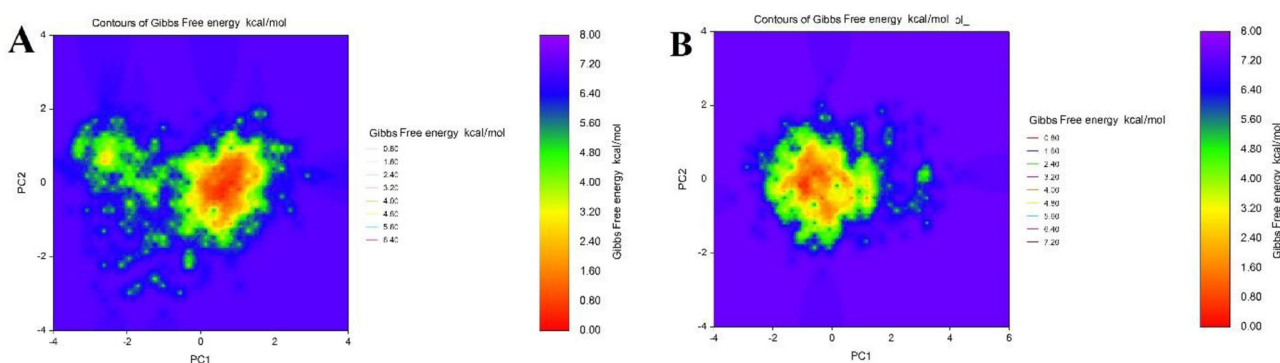


Figure 13. Gibbs free energy landscape calculated from PC1 and PC2 for Neh2 domain (A) WT and (B) L30L mutant.

more stable. The presence of methionine at 565 broadens the energy minimum region, and the white spot indicates that the mutant is a much more energetically stable conformation than WT. In addition, covariance matrix indicated that methionine reduced the correlated movement in the DGR domain from 3.01 to 4.83 nm² (Figure 12(A,B)). Finally, in the Neh2 domain, there is no significant effect of mutation on the dynamic behavior of Neh2 except that WT of Neh2 is a little more stable than mutant peptide (Figure 13), and covariance matrix (Figure 14) 0.461023 to 0.412934 nm² showed a little decrease in movement.

Discussion

Nrf2/Keap1 pathway plays a role in numerous antioxidant pathway cellular redox homeostasis, including the signaling pathway (Baird & Dinkova-Kostova, 2011; Leinonen et al., 2014; Suzuki & Yamamoto, 2015; Zhang, 2010). Nrf2/Keap1 regulates the expression of antioxidant and phase II detoxification enzymes. Nrf2 is a member of the bZIP family of transcription factors (Suzuki & Yamamoto, 2015). Numerous studies in recent years have shown that Nrf2 mediates

anticarcinogenic, neuroprotective and anti-inflammatory effects (Baird & Dinkova-Kostova, 2011; Chu et al., 2018; Kansanen et al., 2013; Kaspar et al., 2009; Kim & Keum, 2016; Leinonen et al., 2014; Suzuki & Yamamoto, 2015; Zhang, 2010; Zhao et al., 2016). These effects are caused by the coordinated effects of the target genes of Nrf2. Nrf2 is highly expressed in tissues where detoxification reactions occur. It is the most important regulator of cellular defense mechanism, especially in many tissues including brain, lung, bladder, kidney, liver, ovarian, macrophages and erythrocytes (Chen et al., 2015; Surh et al., 2008).

Normally, Nrf2 is found in the cytoplasm and interacts with Keap1, an actin binding protein. The Keap1 component is the suppressor of Nrf2 when the cell is not under stress. When the cell is exposed to oxidative stress, it releases Nrf2 to activate cytoprotective genes and to heterodimerize the Maf family with transcription factors (Kensler et al., 2007). With the help of a nuclear localization sequence, the Nrf2 heterodimer quickly binds to the antioxidant responsive element sequence, passing through the nucleus. Thus, transcriptional activation of various cytoprotective genes begins. However, somatic mutations occurring on Nrf2 and/or Keap1

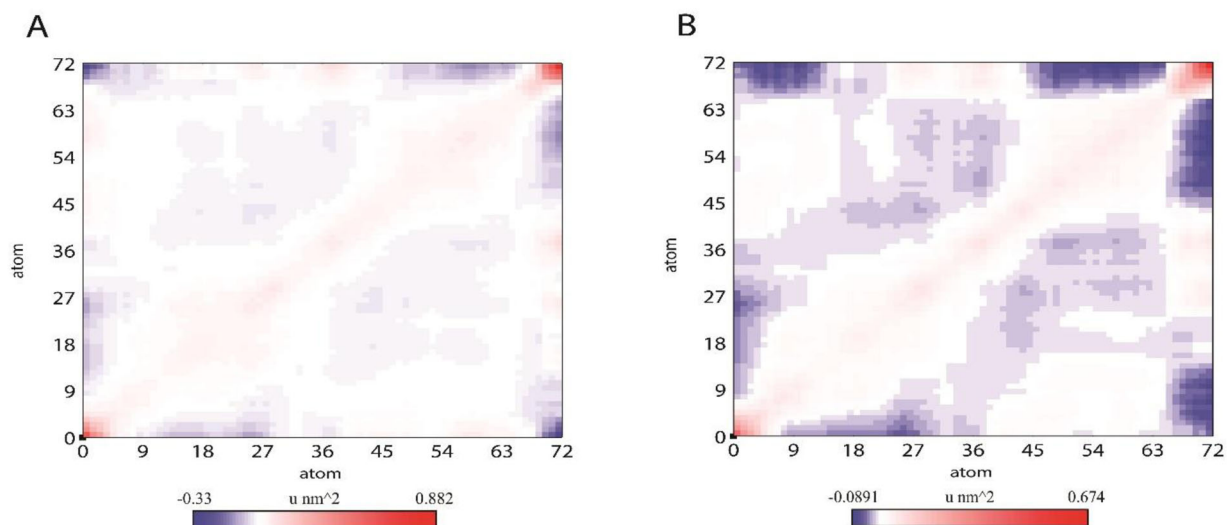


Figure 14. Covariance matrix plot of Nrf2 peptide (A) WT and (B) L30L mutant.

proteins affect these two protein interactions, which can lead to increased nuclear accumulation of Nrf2, resulting in increased cancer cell survival (Bauer et al., 2013; Rushworth et al., 2012). Nrf2 mutations generally affect ETGE and DLG motifs, while Keap1 mutations are distributed more regularly.

In our previous study providing experimental data for this article, DNA mutation analysis was performed for the detection of mutations/SNPs in NF- κ B1, Nrf2, Keap1 and p62 genes in 30 pediatric ALL patients. As a result of mutation analysis in 4 genes in the Nrf2/Keap1/NF- κ B1/p62 signaling pathway, 17 (12 nucleotide changes, 2 deletion mutations and 3 insertions) changes were detected. Six of these changes were first described in this study, and 11 were reported in previous studies. The gene with the most change in study genes is Keap1. During our experimental studies, p.R565fs* 1 somatic pathogenic mutation was detected on the sequences encoding the Kelch/DGR domain in the Keap1 gene. It has been reported that Nrf2 interacts with the Neh2 domain by providing an interaction between Nrf2 and Keap1 when the domain containing this mutation is attached to the Nrf2 actin cytoskeleton. The p.R565M change caused the early termination of translation. We think that Keap1 gene may cause the product, which is 624 amino acids, to terminate at 565 amino acids and cause it to be dysfunctional.

In our study, Keap1 somatic pathogenic p.E121K and p.A159T mutations were detected on the Keap1 BTB domain. This domain is known to be the binding site for the Cul3-E3 dependent ubiquitin ligase complex, which suppresses Nrf2 by promoting Nrf2 ubiquitination and subsequent proteasomal degradation (Mitsuishi et al., 2012; Shibata et al., 2008).

Keap1 contains 27 cysteine residues in humans, which converts the residue protein into a redox sensor for endogenous and environmental oxidative signals as well as for electrophilic reactions. Under normal physiological conditions, oxidation of critical cysteine residues (Cys 151, 273 and 288) on Keap1 with increased ROS or electrophile levels is modified in a tertiary structure, causing Keap1 to separate from Nrf2. 273, 288 and 297 cysteine residues on the Keap1 IVR domain have been reported to be particularly important

for Nrf2 activation and inhibition (Baird & Dinkova-Kostova, 2011; Bauer et al., 2013; Robledinos-Antón et al., 2019).

When comparing Nrf2 genes of different organisms, seven evolutionarily conserved functional homologous domains called Neh (NRF2-ECH homologous domain) have been identified, and these domains are defined as Neh1-7 (Kansanen et al., 2013; Leinonen et al., 2015; Suzuki & Yamamoto, 2015).

Recently, MD simulation studies have been the focus of biologists elucidating the various effects of mutations on proteins, protein-protein interactions, protein-DNA interactions and protein-ligand interactions (Kumar, Bansal, et al., 2019; Sneha et al., 2017). In addition, this powerful method exhibited the best correlation with experimental studies (Benz et al., 2005). Therefore, we hope the present application of a computational platform will explain the effects of mutations, further help in highlighting the potential economic benefit in reducing the cost of experimental analyses and facilitate the tedious process of mutational analysis.

In the current study, comparing WT of BTB domain with its five mutants showed that RMSD value of WT is higher than its mutants. These results are in agreement with those obtained by Karmaj et al. The RMSD results suggested that mutants are more stable compared to native protein (Kamaraj & Purohit, 2013). It is a well-known fact that a proper structure is required for the protein to perform its activity. So, we can say from the RMSD result that mutants are getting more rigid and are altering the protein geometry. For that reason, the protein cannot perform its native function. We did in-depth investigations and used several analysis techniques to understand the fundamental behind these determined single mutations. Our results are in line with our previous study. The RMSF result also suggested that mutation alters structural flexibility. Meanwhile, calculating the FEL provided intimate details about protein folding and energy minima of the proteins (Zhuravlev et al., 2009). The FEL is dependent on the simulation setup, time length, temperature and the number of trajectories run. Thus, the FEL result suggests that the native has a bluer region; so, it is thermodynamically more favorable compared to mutant

protein. The result suggested that mutation inducing the structural changes. BTB domain and its mutants revealed that the WT had the most stable conformations and unfoldable structures. Furthermore, it is clear from RMSD and RMSF of IVR domain that the mutation in 222 with threonine caused an increase in RMSD and increased the flexibility in the backbone of IVR domain. In the DRG domain, due to mutation at 565, the fluctuation in the region 555–570 of DGR causes blocking the binding site of Nrf2 peptide. Similarly, IVR and DRG domain WT had well-defined single local minima, which reflects that WT proteins are more favorable conformations compared to their corresponding mutants. Therefore, the FEL result suggests that the native has a bluer region; so, it is thermodynamically more favorable compared to mutant proteins. The result suggested that mutation induced structural changes. The observed results from MD simulations could be attributed to the pathogenicity of mutants. Meanwhile, the mutation to the Neh2 domain has no significant effect on the RMSD and RMSF of Neh2. In addition, the FEL of Neh2 L30L mutant has no significant thermodynamic effect on the global energy or behavior of resulted mutant compared to WT of Neh2. A possible explanation for this might be the experimental results that revealed that L30L mutant has no pathogenic effect. These results may provide further support for experimental studies.

Conclusion

The present study was designed to determine the structural and dynamical effects of mutants on the general behavior of resulted mutant proteins and to give a complete picture about the secret behind the pathogenicity of mutants. The investigation of RMSD of BTB domain has shown that RMSD of WT has highest RMSD average compared to its corresponding mutants, which indicates that WT of BTB domain is more dynamic. With regard to thermodynamic stability, FEL was assessed for WT and its mutants of BTB showed that the mutants showed less energetic favorability, which explains the reason for them being pathogenic. One of the most significant findings to emerge from this study is that the RMSD for mutants of IVR and DRG domains exhibited increased stability and flexibility of IVR and DGR. Moreover, FEL showed that mutations in both IVR and DGR domains disrupted the global energy of mutants. In the case of Nrf2, the RMSD and RMSF and FEL showed no significant effect on stability, flexibility or energetics of L30L mutant of Neh2. This explains the experimental results of the apathogenic effects of this mutation.

Acknowledgments

We acknowledge the patients and staff who participated in our research studies.

Disclosure statement

No potential conflict of interest was reported by the authors.

References

- Abdul-Aziz, A., MacEwan, D. J., Bowles, K. M., & Rushworth, S. A. (2015). Oxidative stress responses and NRF2 in human leukaemia. *Oxidative Medicine and Cellular Longevity*, 2015, 454659. <https://doi.org/10.1155/2015/454659>
- Abraham, M. J., Murtola, T., Schulz, R., Páll, S., Smith, J. C., Hess, B., & Lindahl, E. (2015). GROMACS: High performance molecular simulations through multi-level parallelism from laptops to supercomputers. *SoftwareX*, 1–2, 19–25. <https://doi.org/10.1016/j.softx.2015.06.001>
- Adzhubei, I. A., Schmidt, S., Peshkin, L., Ramensky, V. E., Gerasimova, A., Bork, P., Kondrashov, A. S., & Sunyaev, S. R. (2010). A method and server for predicting damaging missense mutations. *Nature Methods*, 7(4), 248–249. <https://doi.org/10.1038/nmeth0410-248> <https://doi.org/10.1038/nmeth0410-248>
- Adzhubei, I., Jordan, D. M., & Sunyaev, S. R. (2013). Predicting functional effect of human missense mutations using PolyPhen-2. *Current Protocols in Human Genetics*, 07, Unit7.20. <https://doi.org/10.1002/0471142905.hg0720s76>
- Akın-Balı, D. F., Aktas, S. H., Unal, M. A., & Kankılıç, T. (2020). Identification of novel Nrf2/Keap1 pathway mutations in pediatric acute lymphoblastic leukemia. *Pediatric Hematology and Oncology*, 37(1), 58–75. <https://doi.org/10.1080/08880018.2019.1682090>
- Amadei, A., Linssen, A. B. M., de Groot, B. L., van Aalten, D. M. F., & Berendsen, H. J. C. (1996). An efficient method for sampling the essential subspace of proteins. *Journal of Biomolecular Structure & Dynamics*, 13(4), 615–625. <https://doi.org/10.1080/07391102.1996.10508874>
- Baird, L., & Dinkova-Kostova, A. T. (2011). The cytoprotective role of the Keap1-Nrf2 pathway. *Archives of Toxicology*, 85(4), 241–272. <https://doi.org/10.1007/s00204-011-0674-5>
- Bauer, A. K., Hill, T., & Alexander, C.-M. (2013). The involvement of NRF2 in lung cancer. *Oxidative Medicine and Cellular Longevity*, 2013, 746432. <https://doi.org/10.1155/2013/746432>
- Benz, R. W., Castro-Román, F., Tobias, D. J., & White, S. H. (2005). Experimental validation of molecular dynamics simulations of lipid bilayers: A new approach. *Biophysical Journal*, 88(2), 805–817. <https://doi.org/10.1529/biophysj.104.046821>
- Bjellkmar, P., Larsson, P., Cuendet, M. A., Hess, B., & Lindahl, E. (2010). Implementation of the CHARMM force field in GROMACS: Analysis of protein stability effects from correction maps, virtual interaction sites, and water models. *Journal of Chemical Theory and Computation*, 6(2), 459–466. <https://doi.org/10.1021/ct900549r>
- Bromberg, Y., & Rost, B. (2007). SNAP: Predict effect of non-synonymous polymorphisms on function. *Nucleic Acids Research*, 35(11), 3823–3835. <https://doi.org/10.1093/nar/gkm238>
- Carroll, W. L., & Raetz, E. A. (2012). Clinical and laboratory biology of childhood acute lymphoblastic leukemia. *The Journal of Pediatrics*, 160(1), 10–18. <https://doi.org/10.1016/j.jpeds.2011.08.006>
- Carter, H., Chen, S., Isik, L., Tyekucheva, S., Velculescu, V. E., Kinzler, K. W., Vogelstein, B., & Karchin, R. (2009). Cancer-specific high-throughput annotation of somatic mutations: Computational prediction of driver missense mutations. *Cancer Research*, 69(16), 6660–6667. <https://doi.org/10.1158/0008-5472.CAN-09-1133>
- Carter, H., Douville, C., Stenson, P. D., Cooper, D. N., & Karchin, R. (2013). Identifying Mendelian disease genes with the variant effect scoring tool. *BMC Genomics*, 14(Suppl 3), S3. <https://doi.org/10.1186/1471-2164-14-S3-S3> <https://doi.org/10.1186/1471-2164-14-S3-S3>
- Chen, B., Lu, Y., Chen, Y., & Cheng, J. (2015). The role of Nrf2 in oxidative stress-induced endothelial injuries. *The Journal of Endocrinology*, 225(3), R83–R99. <https://doi.org/10.1530/JOE-14-0662>
- Chu, X.-Y., Z.-J. L., Zheng, Z.-W., Tao, Y.-L., Zou, F.-X., & Yang, X.-F. (2018). KEAP1/NRF2 signaling pathway mutations in cervical cancer. *European Review for Medical and Pharmacological Sciences*, 22(14), 4458–4466. https://doi.org/10.26355/eurrev_201807_15497
- Douville, C., Masica, D. L., Stenson, P. D., Cooper, D. N., Gygax, D. M., Kim, R., Ryan, M., & Karchin, R. (2016). Assessing the pathogenicity of insertion and deletion variants with the variant effect scoring tool (VEST-Indel). *Human Mutation*, 37(1), 28–35. <https://doi.org/10.1002/humu.22911> <https://doi.org/10.1002/humu.22911>

- Frauenfelder, H., Sligar, S. G., & Wolynes, P. G. (1991). The energy landscapes and motions of proteins. *Science (New York, N.Y.)*, 254(5038), 1598–1603. <https://doi.org/10.1126/science.1749933>
- Ganesan, P., & Ramalingam, R. (2019). Investigation of structural stability and functionality of homodimeric gramicidin towards peptide-based drug: A molecular simulation approach. *Journal of Cellular Biochemistry*, 120(4), 4903–4911. <https://doi.org/10.1002/jcb.27765>
- Kamaraj, B., & Purohit, R. (2013). In silico screening and molecular dynamics simulation of disease-associated nsSNP in TYRP1 gene and its structural consequences in OCA3. *BioMed Research International*, 2013, 697051–697051. <https://doi.org/10.1155/2013/697051>
- Kansanen, E., Kuosmanen, S. M., Leinonen, H., & Levenon, A.-L. (2013). The Keap1-Nrf2 pathway: Mechanisms of activation and dysregulation in cancer. *Redox Biology*, 1(1), 45–49. <https://doi.org/10.1016/j.redox.2012.10.001> <https://doi.org/10.1016/j.redox.2012.10.001>
- Kaspar, J. W., Niture, S. K., & Jaiswal, A. K. (2009). Nrf2:INrf2 (Keap1) signaling in oxidative stress. *Free Radical Biology & Medicine*, 47(9), 1304–1309. <https://doi.org/10.1016/j.freeradbiomed.2009.07.035>
- Kensler, T. W., Wakabayashi, N., & Biswal, S. (2007). Cell survival responses to environmental stresses via the Keap1-Nrf2-ARE pathway. *Annual Review of Pharmacology and Toxicology*, 47(1), 89–116. <https://doi.org/10.1146/annurev.pharmtox.46.120604.141046>
- Kerins, M. J., & Ooi, A. (2018). A catalogue of somatic NRF2 gain-of-function mutations in cancer. *Scientific Reports*, 8(1), 12846. <https://doi.org/10.1038/s41598-018-31281-0>
- Khan, M. T., Khan, A., Rehman, A. U., Wang, Y., Akhtar, K., Malik, S. I., & Wei, D.-Q. (2019). Structural and free energy landscape of novel mutations in ribosomal protein S1 (rpsA) associated with pyrazinamide resistance. *Scientific Reports*, 9(1), 7482. <https://doi.org/10.1038/s41598-019-44013-9>
- Kim, J., & Keum, Y. S. (2016). NRF2, a key regulator of antioxidants with two faces towards cancer. *Oxidative Medicine and Cellular Longevity*, 2016, 2746457. <https://doi.org/10.1155/2016/2746457>
- Kumar, N., Gupta, S., Chand Yadav, T., Pruthi, V., Kumar Varadwaj, P., & Goel, N. (2019). Extrapolation of phenolic compounds as multi-target agents against cancer and inflammation. *Journal of Biomolecular Structure & Dynamics*, 37(9), 2355–2369. <https://doi.org/10.1080/07391102.2018.1481457>
- Kumar, R., Bansal, A., Shukla, R., Raj Singh, T., Wasudeo Ramteke, P., Singh, S., & Gautam, B. (2019). In silico screening of deleterious single nucleotide polymorphisms (SNPs) and molecular dynamics simulation of disease associated mutations in gene responsible for oculocutaneous albinism type 6 (OCA 6) disorder. *Journal of Biomolecular Structure & Dynamics*, 37(13), 3513–3523. <https://doi.org/10.1080/07391102.2018.1520649>
- Leinonen, H. M., Kansanen, E., Pölonen, P., Heinäniemi, M., & Levenon, A.-L. (2014). Chapter Eight - Role of the Keap1-Nrf2 pathway in cancer. In D. M. Townsend & K. D. Tew (Eds.), *Advances in cancer research* (Vol. 122, pp. 281–320). Academic Press.
- Leinonen, H. M., Kansanen, E., Pölonen, P., Heinäniemi, M., & Levenon, A.-L. (2015). Dysregulation of the Keap1-Nrf2 pathway in cancer. *Biochemical Society Transactions*, 43(4), 645–649. <https://doi.org/10.1042/BST20150048>
- Liu, H., & Yao, X. (2010). Molecular basis of the interaction for an essential subunit PA-PB1 in influenza virus RNA polymerase: Insights from molecular dynamics simulation and free energy calculation. *Molecular Pharmaceutics*, 7(1), 75–85. <https://doi.org/10.1021/mp900131p>
- Mitsuishi, Y., Motohashi, H., & Yamamoto, M. (2012). The Keap1-Nrf2 system in cancers: Stress response and anabolic metabolism. *Frontiers in Oncology*, 2, 200. <https://doi.org/10.3389/fonc.2012.00200>
- Mullighan, C. G. (2014). The genomic landscape of acute lymphoblastic leukemia in children and young adults. *Hematology - American Society of Hematology Education Program*, 2014(1), 174–180. <https://doi.org/10.1182/asheducation-2014.1.174>
- Mullighan, C. G., & Downing, J. R. (2009). Genome-wide profiling of genetic alterations in acute lymphoblastic leukemia: Recent insights and future directions. *Leukemia*, 23(7), 1209–1218. <https://doi.org/10.1038/leu.2009.18>
- Narang, S. S., Shuaib, S., Goyal, D., & Goyal, B. (2018). Assessing the effect of D59P mutation in the DE loop region in amyloid aggregation propensity of β 2-microglobulin: A molecular dynamics simulation study. *Journal of Cellular Biochemistry*, 119(1), 782–792. <https://doi.org/10.1002/jcb.26241>
- Pui, C. H., & Evans, W. E. (1998). Acute lymphoblastic leukemia. *The New England Journal of Medicine*, 339(9), 605–615. <https://doi.org/10.1056/NEJM199808273390907>
- Robledinos-Antón, N., Fernández-Ginés, R., Manda, G., & Cuadrado, A. (2019). Activators and inhibitors of NRF2: A review of their potential for clinical development. *Oxidative Medicine and Cellular Longevity*, 2019, 9372182. <https://doi.org/10.1155/2019/9372182>
- Rushworth, S. A., Zaitseva, L., Murray, M. Y., Shah, N. M., Bowles, K. M., & MacEwan, D. J. (2012). The high Nrf2 expression in human acute myeloid leukemia is driven by NF- κ B and underlies its chemo-resistance. *Blood*, 120(26), 5188–5198. <https://doi.org/10.1182/blood-2012-04-422121>
- Shibata, T., Ohta, T., Tong, K. I., Kokubu, A., Odogawa, R., Tsuta, K., Asamura, H., Yamamoto, M., & Hirohashi, S. (2008). Cancer related mutations in NRF2 impair its recognition by Keap1-Cul3 E3 ligase and promote malignancy. *Proceedings of the National Academy of Sciences of the United States of America*, 105(36), 13568–13573. <https://doi.org/10.1073/pnas.0806268105> <https://doi.org/10.1073/pnas.0806268105>
- Shukla, R., Munjal, N. S., & Singh, T. R. (2019). Identification of novel small molecules against GSK3 β for Alzheimer's disease using chemoinformatics approach. *Journal of Molecular Graphics & Modelling*, 91, 91–104. <https://doi.org/10.1016/j.jmkgm.2019.06.008>
- Sneha, P., Thirumal Kumar, D., Priya Doss, C. G., Siva, R., & Zayed, H. (2017). Determining the role of missense mutations in the POU domain of HNF1A that reduce the DNA-binding affinity: A computational approach. *PLoS One*, 12(4), e0174953. <https://doi.org/10.1371/journal.pone.0174953>
- Surh, Y. J., Kundu, J. K., & Na, H. K. (2008). Nrf2 as a master redox switch in turning on the cellular signaling involved in the induction of cytoprotective genes by some chemopreventive phytochemicals. *Planta Medica*, 74(13), 1526–1539. <https://doi.org/10.1055/s-0028-1088302>
- Suzuki, T., & Yamamoto, M. (2015). Molecular basis of the Keap1-Nrf2 system. *Free Radical Biology & Medicine*, 88(Pt B), 93–100. <https://doi.org/10.1016/j.freeradbiomed.2015.06.006>
- Tate, J. G., Bamford, S., Jubb, H. C., Sondka, Z., Beare, D. M., Bindal, N., Boutselakis, H., Cole, C. G., Creatore, C., Dawson, E., Fish, P., Harsha, B., Hathaway, C., Jupe, S. C., Kok, C. Y., Noble, K., Ponting, L., Ramshaw, C. C., Rye, C. E., ... Forbes, S. A. (2019). COSMIC: The catalogue of somatic mutations in cancer. *Nucleic Acids Research*, 47(D1), D941–D947. <https://doi.org/10.1093/nar/gky1015>
- Walters-Sen, L. C., Hashimoto, S., Thrush, D. L., Reshmi, S., Gastier-Foster, J. M., Astbury, C., & Pyatt, R. E. (2015). Variability in pathogenicity prediction programs: Impact on clinical diagnostics. *Molecular Genetics & Genomic Medicine*, 3(2), 99–110. <https://doi.org/10.1002/mggg.3.116>
- Wang, Y., Miller, S., Roulston, D., Bixby, D., & Shao, L. (2016). Genome-wide single-nucleotide polymorphism array analysis improves prognostication of acute lymphoblastic leukemia/lymphoma. *The Journal of Molecular Diagnostics: JMD*, 18(4), 595–603. <https://doi.org/10.1016/j.jmoldx.2016.03.004>
- Wong, W. C., Kim, D., Carter, H., Diekhans, M., Ryan, M. C., & Karchin, R. (2011). CHASM and SNVBox: Toolkit for detecting biologically important single nucleotide mutations in cancer. *Bioinformatics*, 27(15), 2147–2148. <https://doi.org/10.1093/bioinformatics/btr357> <https://doi.org/10.1093/bioinformatics/btr357>
- Zhang, D. D. (2010). The Nrf2-Keap1-ARE signaling pathway: The regulation and dual function of Nrf2 in cancer. *Antioxidants & Redox Signaling*, 13(11), 1623–1626. <https://doi.org/10.1089/ars.2010.3301>
- Zhang, H.-H., Wang, H.-S., Qian, X.-W., Fan, C.-Q., Li, J., Miao, H., Zhu, X.-H., Yu, Y., Meng, J.-H., Cao, P., Le, J., Jiang, J.-Y., Jiang, W.-J., Wang, P., & Zhai, X.-W. (2019). Genetic variants and clinical significance of pediatric acute lymphoblastic leukemia. *Annals of Translational Medicine*, 7(14), 3.
- Zhao, H., Hao, S., Xu, H., Ma, L., Zhang, Z., Ni, Y., & Yu, L. (2016). Protective role of nuclear factor erythroid 2-related factor 2 in the hemorrhagic shock-induced inflammatory response. *International Journal of Molecular Medicine*, 37(4), 1014–1022. <https://doi.org/10.3892/ijmm.2016.2507>
- Zhuravlev, P. I., Materese, C. K., & Papoian, G. A. (2009). Deconstructing the native state: Energy landscapes, function, and dynamics of globular proteins. *The Journal of Physical Chemistry B*, 113(26), 8800–8812. <https://doi.org/10.1021/jp810659u>